J. Fluid Mech. (1997), *vol.* 338, *pp.* 157–172

Absolute and convective instabilities of plane turbulent wakes in a shallow water layer

By DAOYI CHEN[1] AND GERHARD H. JIRKA[2]

[1] Hydrodynamics Research Group, School of Engineering, University of Manchester, M13 9PL, UK

[2] Institute of Hydromechanics, University of Karlsruhe, Germany

(Received 20 June 1996 and in revised form 12 December 1996)

In shallow turbulent wake flows (typically an island wake), the flow patterns have been found experimentally to depend mainly on a shallow wake parameter, $S = c_f D/h$ in which c_f is a quadratic-law friction coefficient, D is the island diameter and h is water depth. In order to understand the dependence of flow patterns on S, the shallow-water stability equation (a modified Orr–Sommerfeld equation) has been derived from the depth-averaged equations of motion with terms which describe bottom friction. Absolute and convective instabilities have been investigated on the basis of wake velocity profiles with a velocity deficit parameter R. Numerical computations have been carried out for a range of R-values and a stability diagram with two dividing lines was obtained, one defining the boundary between absolute and convective instabilities S_{ca}, and another defining the transition between convectively unstable and stable wake flow S_{cc}. The experimental measurements (Chen & Jirka 1995) of return velocities in shallow wakes were used to compute R-values and two critical values, $S_A = 0.79$ and $S_C = 0.85$, were obtained at the intersections with lines S_{ca} and S_{cc}. Through comparison with transition values observed experimentally for wakes with unsteady bubble (recirculation zone) and vortex shedding, S_U and S_V respectively, the sequence $S_C > S_A > S_U > S_V$ shows vortex shedding to be the end product of absolute instability. This is analogous to the sequence of critical Reynolds numbers for an unbounded wake of large spanwise extent. Experimental frequency characteristics compare well with theoretical results. The observed values of S_U and S_V for different flow patterns correspond to the velocity profile with $R = -0.945$, which is located at the end of the wake bubble, and it provides the dominant mode.

1. Introduction

Previous work has revealed characteristic features of the so-called 'shallow wake' in geophysical and environmental flows. One typical example is the island wake in which both 'vortex street' and 'stable bubble wakes' have been visualized through the aerial photographs of Van Dyke (1982), Wolanski, Imberger & Heron (1984), Pattiaratchi, James & Collins (1986), and Ingram & Chu (1987). The phenomena of both bubble and vortex wakes have also been observed downwind of mountains in the atmosphere (Scorer 1978; Smith & Grubisic 1993). Chen & Jirka (1995) studied this kind of flow experimentally on a shallow water table. The 'shallow wake' was generated by vertical cylindrical bodies extending over the water depth. The ambient flow is characterized by two main features: one is the existence of a free surface and bottom by which the shallow water layer is bounded and the other is a fully developed turbulent boundary layer. Here the transverse body dimension D greatly exceeds the water depth $h (D/h \gg 1)$.

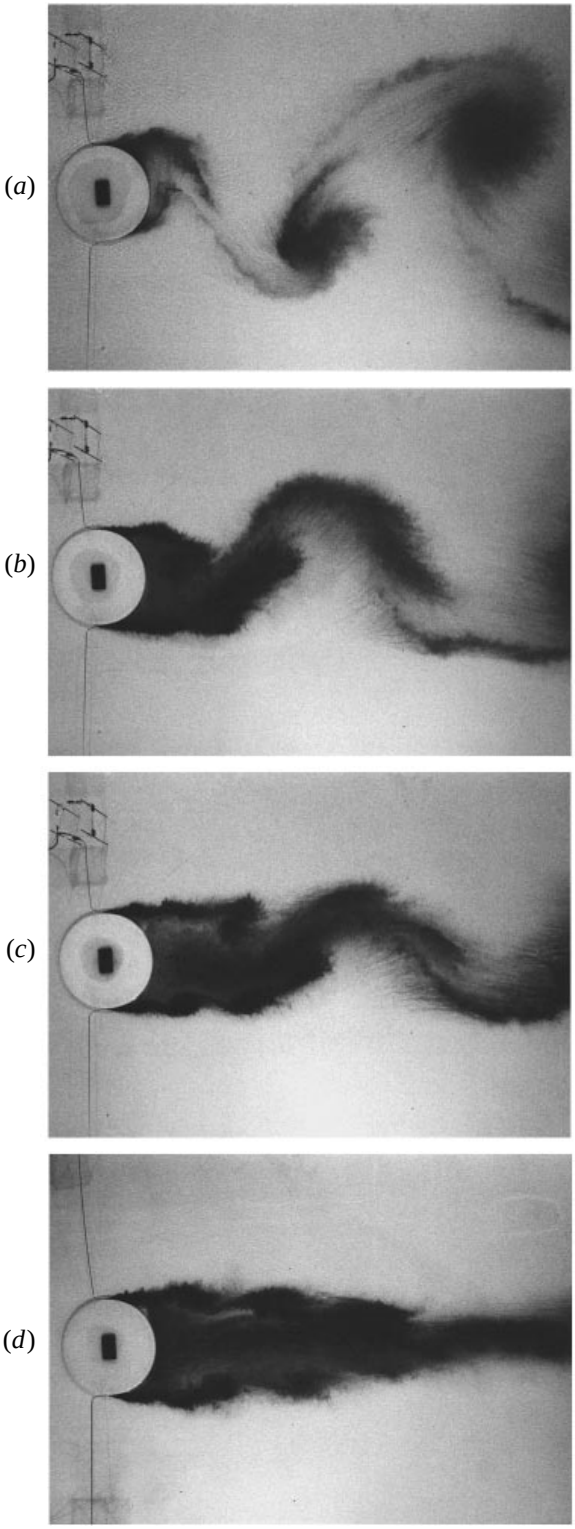

FIGURE 1. Schematic flow patterns of a shallow near wake produced by a $D = 62$ cm cylinder (adapted from figure 5 of Chen & Jirka 1995): (*a*) vortex street pattern ($S = 0.19$, $Re_h = 5900$,

The wake Reynolds number $Re_d = U_a D/\nu$ was very large, greater than 10^4, while the ambient flow Reynolds number that governs the shear flow in the transverse dimension $Re_h = U_a h/\nu$ was always larger than 1500. U_a is the depth-average ambient velocity and ν is the kinematic viscosity. Re_h is thus well above the transition value of about 500. Different types of body were investigated, including cylinders, flat plates and porous plates oriented transversely to the ambient flow. The flow patterns fell into three categories: vortex shedding, unsteady bubble and steady bubble as shown in figure 1. A stability parameter $S = c_f D/h$ has been used to classify these three flow patterns. The friction coefficient of the water table c_f was estimated from the standard smooth-wall relation.

An important challenge is to explain the evolution of these flow patterns. The presence of background turbulence makes the shallow wake greatly different from unbounded low-Reynolds-number wakes which have been studied previously (e.g. Roshko 1961; Morkovin 1964; Gerrard 1978). For instance, in shallow water either vortex shedding or a stable wake could be observed for wake Reynolds number values from 10^4 (in the experiments) to 10^7 (in nature), while vortex shedding always occurs in unbounded wakes when the Reynolds number is of the order of 100. In the shallow wake, stabilization is due to bottom friction as well as the kinematical restriction in the vertical direction.

To obtain a theoretical explanation for the shallow wake instability we consider here the analysis of absolute and convective instabilities made in relation to von Kármán vortex shedding from unbounded two-dimensional bodies. The concept of absolute and convective instability was first defined in plasma physics by Briggs (1964) and Bers (1975). Traditional instability analysis had previously dealt with the spatial mode (real frequency) and the temporal mode (real wavenumber) separately. Absolute and convective instabilities concern temporal–spatial problems (complex wavenumber and frequency) and provide the theoretical insight needed to classify free shear flows. For example, the mixing layer, the pure jet, and the far wake are convectively unstable under normal conditions (e.g. uniform density, no external forcing) since only spatial evolution of a disturbance is possible. However, a part of the near-wake flow is absolutely unstable and a temporal growth of a disturbance results in vortex shedding, which is the saturated end product of this temporal global instability.

Related work on absolute and convective instabilities in unbounded wake flows can be traced back to Betchov & Criminale (1966). They discovered a branch-point singularity of the inviscid dispersion relation in the upper complex-frequency plane indicating absolute instability for a wake profile with zero centreline velocity. Reviews on the topic of absolute instability can be found in Huerre & Monkewitz (1990) and Oertel (1990). Among previous works, it is noted that Monkewitz (1988) studied the effect of Reynolds number on local absolute instability and Chomaz, Huerre & Redekopp (1988, 1991) have studied the global instabilities of wakes.

With regard to shallow wake flows, Schar & Smith (1993) studied the global normal mode of instability for an inviscid flow pass an isolated topography. Grubisic, Smith & Schar (1995) carried out a local absolute stability analysis for a piecewise-linear velocity profile which unfortunately missed the two inflection points. The reverse flow velocity was determined by the magnitude of bottom friction which also defined the velocity profile. A surface drag number r was defined as the product of the drag coefficient and the ratio of horizontal length scale and the height of fluid layer. (This

$Re_d = 183000$); (*b*) unsteady bubble wake ($S = 0.27$, $Re_h = 3810$, $Re_d = 149000$); (*c*) unsteady bubble wake with weaker downstream instabilities ($S = 0.34$, $Re_h = 2600$, $Re_d = 115000$); and (*d*) steady bubble wake ($S = 0.53$, $Re_h = 1800$, $Re_d = 112000$).

definition is analogous to the wake stability parameter S given above but differs by a factor of 2 due to the choice of the drag coefficient.) A critical value of $r = 0.1$ was obtained from their stability analysis.

The purpose of this paper on shallow wakes is to investigate the effect of bottom friction on the absolute and convective stability characteristics of wake flows by means of a linear stability analysis, and thus interpret and compare with the results of our earlier experimental study (Chen & Jirka 1995). General velocity profiles are used and bottom friction is considered over a wide parameter range. According to the experimental results of Chen & Jirka (1995), the reverse velocity remains almost constant in vortex shedding and unsteady bubble wakes within a wide range of bottom friction parameter when $S < 0.6$, but decreases gradually in the steady bubble wake with increasing S. For this reason, we consider the variation of both reverse velocity and bottom friction. Some preliminary results of this analysis had been presented by Chen & Jirka (1993).

2. Linear instability characteristics of shallow wake flows

In this section, the shallow wake flow behaviour is investigated by means of a linear instability analysis of the two-dimensional depth-averaged equations of motion with bottom friction terms. The base flow is assumed to be parallel. Both absolute and convective instability characteristics and their dependence on the shallow wake parameter S are explored.

Obviously, given the complicated character of the near-wake recirculating flow and the gradual evolution in the far wake, the results of such calculations can at best approximate reality. Nevertheless, it has been shown by earlier applications of this technique to unbounded wake flows (for example, see Huerre & Monkewitz 1990) that they can explain qualitatively many of the observed wake features.

2.1. *The shallow-water stability equation with bottom friction*

In a shallow water layer, the depth-averaged equations of motion for parallel slightly disturbed flow with the two-dimensional (x, y) velocity field $(U+u, v)$ (see Chu, Wu & Khayat 1991), in which $U(y)$ is the base velocity and $u(x, y, t)$ and $v(x, y, t)$ are the disturbance velocities, and p is the disturbance pressure, are:

$$\frac{\partial u}{\partial x}+\frac{\partial v}{\partial y}=0, \tag{1}$$

$$\frac{\partial u}{\partial t}+U\frac{\partial u}{\partial x}+v\frac{\partial U}{\partial y}=-\frac{1}{\rho}\frac{\partial p}{\partial x}-\frac{c_f U}{h}u+\epsilon_h \nabla^2 u, \tag{2}$$

$$\frac{\partial v}{\partial t}+U\frac{\partial v}{\partial x}=-\frac{1}{\rho}\frac{\partial p}{\partial y}-\frac{c_f U}{2h}v+\epsilon_h \nabla^2 v \tag{3}$$

in which ρ is the density, c_f the turbulent friction coefficient and ϵ_h the horizontal eddy diffusivity.

The small-amplitude velocity disturbances are harmonic in x, t:

$$u=\phi_u(y)\,\mathrm{e}^{\mathrm{i}(\alpha x-\beta t)}, \tag{4}$$

$$v=\phi_v(y)\,\mathrm{e}^{\mathrm{i}(\alpha x-\beta t)}, \tag{5}$$

in which ϕ_u and ϕ_v are complex amplitude functions. Furthermore, $\alpha=\alpha_r+\mathrm{i}\alpha_i$, where α_r is the wavenumber of the disturbance, and $-\alpha_i$ is the spatial amplification rate for

modes that propagate in the $x > 0$ direction, while $+\alpha_i$ is the spatial amplification rate for modes that propagate in the $x < 0$ direction, and $\beta = \beta_r + \mathrm{i}\beta_i$, where β_r is the frequency of the disturbance, and β_i the temporal amplification rate.

Substituting these terms into the depth-averaged equations of motions leads to

$$i\alpha\phi_u = -\phi_v', \tag{6}$$

$$\mathrm{i}\alpha(U-C)\,\phi_u - U'\phi_v + \mathrm{i}\alpha p = -\frac{c_f U}{h}\phi_u + \epsilon_h(\phi_u'' - \alpha^2\phi_u), \tag{7}$$

$$\mathrm{i}\alpha(U-C)\,\phi_v + p' = -\frac{c_f U}{h}\phi_v + \epsilon_h(\phi_v'' - \alpha^2\phi_v), \tag{8}$$

where the prime denotes differentiation with respect to the transverse coordinate y. $C = \beta/\alpha = C_r + \mathrm{i}C_i$, where C_r is the phase speed. After eliminating the pressure and ϕ_u, one obtains the shallow-water stability equation with bottom friction (dropping the subscript on ϕ_v)

$$(U(y) - C + \xi)(\phi'' - \alpha^2\phi) + \xi\frac{U'}{U}\phi' - U''\phi = \epsilon_h(\phi'''' - 2\alpha^2\phi'' + \alpha^4\phi), \tag{9}$$

where $\xi = c_f U/(\mathrm{i}\alpha h) = S_l/(\mathrm{i}\alpha\, 2l)$ is a parameter measuring the effect of local friction and $S_l = c_f 2l/h$ is the local wake stability parameter in which l is the local wake half-width. The boundary conditions are

$$\phi(\pm l_0) = \phi'(\pm l_0) = 0, \tag{10}$$

where ϕ is the eigenfunction which represents the amplitude of the disturbance in the y-direction. Two sidewalls are located at $y = l_0$ and $-l_0$, where $l_0 \to \infty$. Equation (9) is a modified form of the Orr–Sommerfeld equation with the added effect of bottom friction.

2.2. *Search procedure for absolute and convective instabilities*

As has been mentioned in the Introduction, Betchov & Criminale (1966) discovered a branch-point singularity of the inviscid dispersion relation in the upper complex-frequency plane for a wake profile with zero centreline velocity. This branch point indicates the existence of absolute instability. The characteristics of the absolute and convective instability in shear flows can be determined by investigation of its impulse response (see Monkewitz, 1988). An impulse contains modes of all frequency and wavenumbers. A given flow may amplify the unstable modes. If one introduces a Green's function $G(x, t)$ to represent the impulse response, the Green's function takes on the form of a wave packet in the (x, t)-plane. For each ray $x/t =$ constant, the impulse mode with wavenumber α^* is given by

$$\frac{\mathrm{d}\beta}{\mathrm{d}\alpha}(\alpha^*) = \frac{x}{t}. \tag{11}$$

The quantity $\mathrm{d}\beta/\mathrm{d}\alpha$ at the saddle point is constant along rays of constant x/t, and since x/t is real. Moving along a ray with velocity $\mathrm{d}\beta/\mathrm{d}\alpha$ at the saddle point, the wave given by α^* and β^* grows temporally with a growth rate given by

$$\sigma_i = \beta_i(\alpha^*) - \alpha_i^*\frac{\mathrm{d}\beta}{\mathrm{d}\alpha}(\alpha^*). \tag{12}$$

Whenever at a certain point the condition of the group velocity $\mathrm{d}\beta/\mathrm{d}\alpha = 0$ is satisfied, an absolute growth rate σ_i that corresponds to α^* is given as $\sigma_i = \beta_i(\alpha^*)$. If $\beta_i > 0$, there will exist unstable modes travelling upstream relative to the location of the

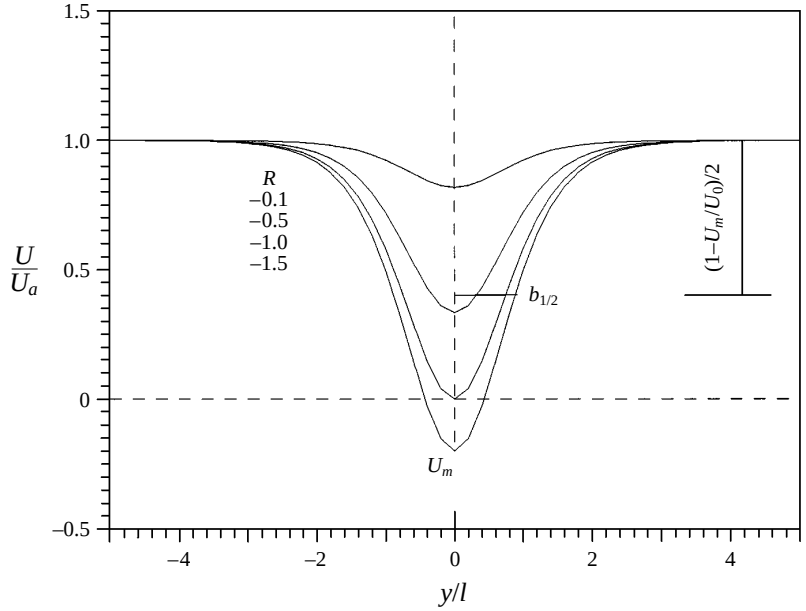

FIGURE 2. Definition of wake velocity profiles.

disturbance and the flow may be referred to as *absolute unstable*. Conversely, for $\beta_i < 0$, the flow is *convectively unstable*, and the unstable modes will be travelling downstream only.

Searching in the (α, β) domain for the saddle point, where $\mathrm{d}\beta/\mathrm{d}\alpha = 0$, may provide the criterion to distinguish whether the flow is absolutely or convectively unstable. For example, $\mathrm{d}\beta/\mathrm{d}\alpha = 0$ with $\beta_i > 0$ is satisfied at a pinch-type branch point, which separates into the upper and lower halves of the complex α-plane when β_i tends to infinity. This was found by Betchov & Criminale (1966) for the wake flow with zero velocity on the centreline, so this wake flow is absolutely unstable.

In the present work, an improved eigenvalue searching procedure by means of the Chebyshev pseudospectral technique has been used to solve accurately and efficiently the shallow-water stability equation with the bottom friction terms. This technique has been described in Chen & Jirka (1994).

The transverse velocity profile of a self-preserving wake may be approximated by (Monkewitz 1988)

$$U(y) = \bar{U}(1 - R + 2\,\mathrm{sech}^2\, R(y/l)) \tag{13}$$

as sketched in figure 2 where $R = (U_m - U_a)/(U_m + U_a)$ is the velocity ratio, $\bar{U} = \frac{1}{2}(U_m + U_a)$ is the mean wake velocity, U_a is the ambient velocity, U_m is the wake centreline velocity, and l is the transverse length scale (l is related to the half-width $b = \sinh^{-1}(1)$ $l = 0.881\, l$ as shown in figure 2). $R = 0$ means uniform flow, $R = -1$ is a wake with zero centreline velocity, and $R < -1$ means reverse flow on the centreline. In an actual developing wake flow behind a bluff body, R gradually increases with distance downstream from negative values towards zero at large distances.

Equation (13) is the special case of the more general wake profile definition used by Monkewitz (1988), $U(y) = \bar{U}(1 - R + 2R[1 + \sinh^{2N}(y/l)]^{-1}$ with $N = 1$. For $N > 1$, this provides flatter profiles in the wake centre. From Monkewitz's work for unbounded plane wakes (his figure 2) it is apparent that, for near-wake values when $R \leqslant -1$, the value of the Reynolds number (based on kinematic viscosity) dividing absolute and

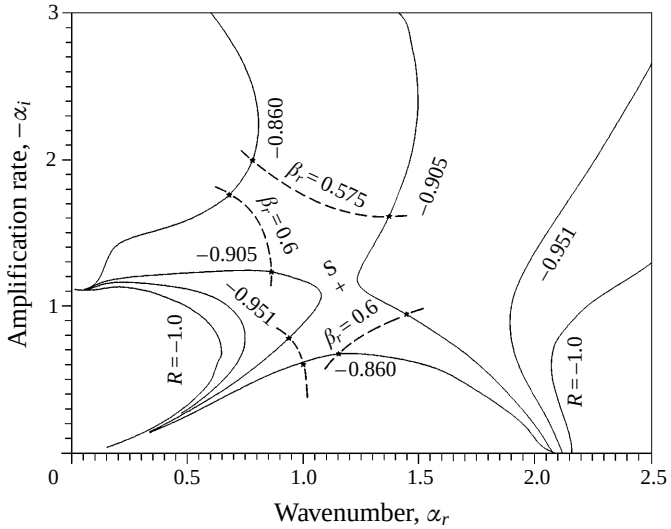

FIGURE 3. Eigenvalues of sinuous modes of instabilities for the inviscid wake ($Re_b \to \infty$) and without bottom friction ($S_b = 0$). Solid lines refer to different velocity ratios R. Values of the frequency β_r are shown around the saddle point only. The saddle point S refers to the absolute/convective instability transition.

convective instability changes only slightly over the range $1 < N < 5$ and the minimum Reynolds number lies in this range. On the other hand, for far-wake values, $R \geqslant -1$, the wake flow approaches $N = 1$. For this reason the special form of (13) was retained for all calculations since we have the primary aim of investigating the dependence of shallow wake characteristics on the additional parameter $S_b = c_f 2b/h$.

An example of the validation and accuracy of the present search procedure is given in figure 3 for the unbounded inviscid wake without any bottom friction. Assuming $\beta_i = 0$, a number of curves for constant R can be obtained and are shown on the $(\alpha_r, -\alpha_i)$-plane. It is found that a saddle point exists at $R = -0.904$ and with $\beta_r = 0.591$. These results are in exact agreement with the earlier computations of Mattingly & Criminale (1972) and of Monkewitz & Nguyen (1987). This means that the wake flow is absolutely unstable for $R < -0.904$ and convectively unstable for $R > -0.904$.

Because the varicose mode shows no signs of absolute instability for the range of realistic wake flow profiles (see Monkewitz & Nguyen 1987), and because the wake flow generally is more susceptible to sinuous instabilities, the following results only deal with the sinuous mode.

2.3. *Numerical results for shallow wake flows*

Transition from absolutely unstable to convectively unstable flows. In figure 4 the case of inviscid ($\epsilon_h = 0$) flow with a velocity profile $R = -1$ is explored. (Note that $R = -1$ is less than the critical value $R = -0.904$ that divides absolute and convective instabilities for the case of no bottom friction, as represented in figure 3.) Thus, assuming $\beta_i = 0$, which is the dividing line between an absolute and a convective unstable mode, a series of eigenvalues can be found that represent the wake friction parameter S_b and the frequency β_r as contours in the $(\alpha_r, -\alpha_i)$-plane. The saddle point, with $S_b = 0.331$, frequency $\beta_r = 0.558$, wavenumber $\alpha_r = 1.36$ and $\alpha_i = -0.68$, is a particular pinch-type branch point at which there is a group velocity $\mathrm{d}\beta/\mathrm{d}\alpha = 0$ with $\beta_i = 0$. As discussed above, when the group velocity $\mathrm{d}\beta/\mathrm{d}\alpha = 0$, $\beta_i > 0$ indicates that the flow is absolutely unstable and $\beta_i < 0$ that it is convectively unstable. Therefore, the group

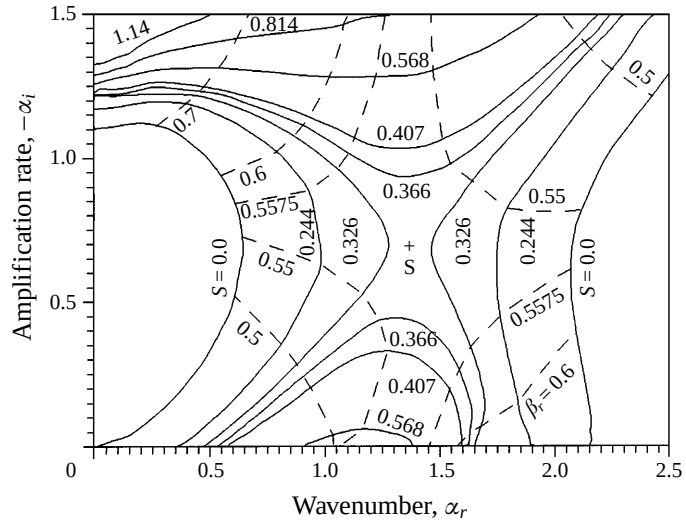

FIGURE 4. Eigenvalues of sinuous modes of instabilities for the shallow wake with velocity ratio $R = -1$ and with inviscid conditions ($Re_b \to \infty$). Solid lines refer to different values of the wake parameter S_b; dashed lines to the frequency β_r. Saddle point S refers to the absolute/convective instability transition.

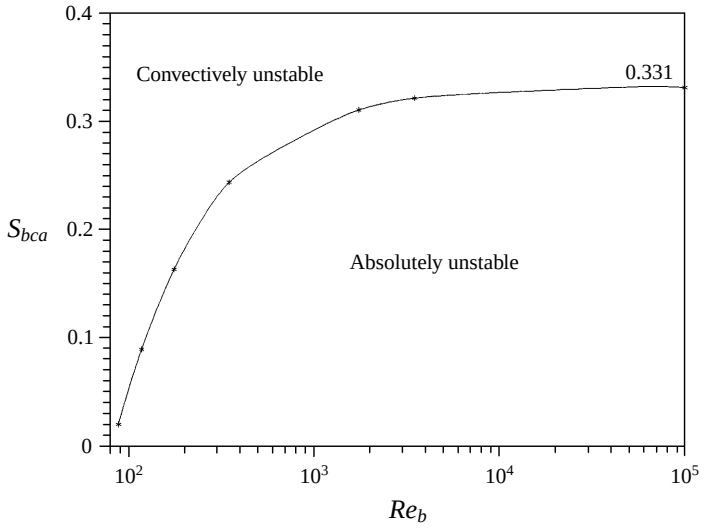

FIGURE 5. Joint effect of wake Reynolds number Re_b and wake friction parameter S_b on the absolute/convective instability transition in the shallow wake with velocity ratio of $R = -1.0$. The asymptotic inviscid transition is $S_{bca} = 0.331$.

velocity $\mathrm{d}\beta/\mathrm{d}\alpha = 0$ with $\beta_i = 0$ at the saddle point is the dividing line of absolute and convective instability. The value of $S_b = 0.331$ is defined as the critical wake friction parameter S_{bca} for the velocity profile with $R = -1$.

The combined effect of bottom friction, expressed by the wake parameter S_b, and of the horizontal diffusion coefficient, expressed by the wake Reynolds number $Re_b = U_a 2b/\epsilon_h$, is shown in figure 5. The asymptote for $Re_b \to \infty$ is given by the critical value $S_{bca} = 0.331$ shown in figure 5. The decrease in S_{bca} with increasing diffusion coefficient (decreasing Re_b) is very gradual to about $S_{bca} = 0.3$ at $Re_b = 1000$. As will

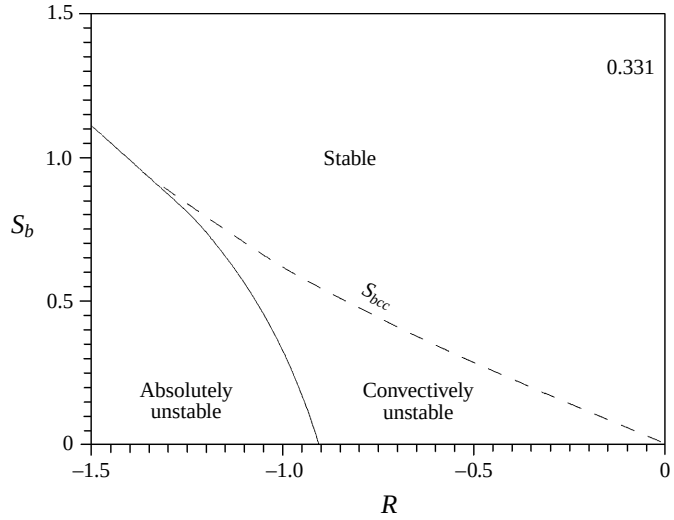

FIGURE 6. Stability diagram for the shallow wake under inviscid conditions showing absolutely unstable, convectively unstable, and stable domains as a function of velocity ratio R and wake friction parameter S_b.

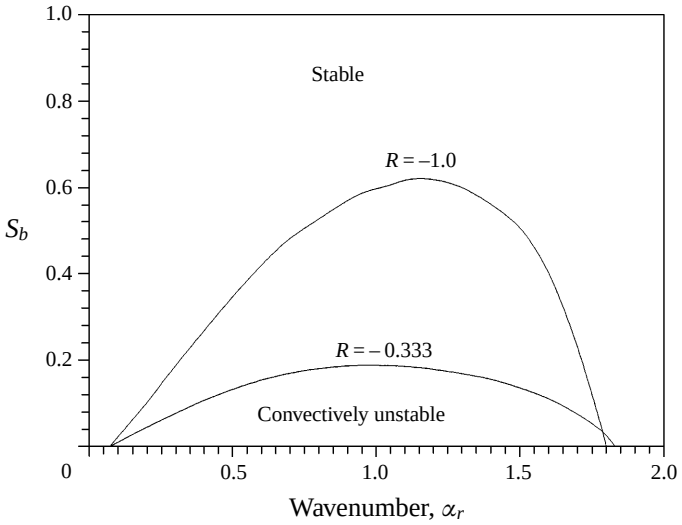

FIGURE 7. Convective instability to stable flow transition in the shallow wake for two values of velocity ratio R as a function of wavenumber α_r and wake friction parameter S_b.

be shown in the next section, typical values for the turbulent wake Reynolds number Re_b are very large ($> 10^3$) for wide shallow wakes so that the inviscid assumption ($Re_b \to \infty$) will be a very good indication of the wake instability characteristics, and will be adopted in the following analysis.

Calculations for selected velocity profiles in the range $-0.904 > R > -1.5$ reveal the dependence of the absolute/convective instability boundary condition S_{bca} on R, which is shown in figure 6. From these results, it is found that bottom friction does damp the absolute instability in near-wake flows. At least qualitatively, this effect is similar to that of viscosity in unbounded wakes (Monkewitz 1988) and of density in hot unbounded jets (Yu & Monkewitz 1988).

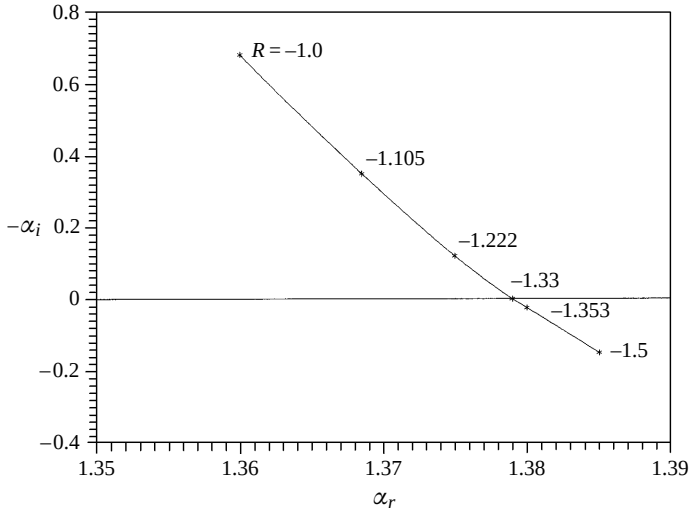

FIGURE 8. Locations in the $(\alpha_r, -\alpha_i)$-domain of the saddle points indicating absolute/convective instability transition for different velocity ratios R.

Transition from convectively unstable to stable flows. Referring to figure 4, when $S_b > S_{bca} = 0.331$, one may find a pair of curves for each S_b-value: one curve is located above the saddle point and the other below it. The upper curve corresponds to a spatially damped upstream-propagating mode. The lower curve, however, moves down with increasing S_b, attaining a maximum value of the spatial amplification rate $-\alpha_i$ equal to zero at $S_b = 0.618$. This marginal value indicates the damping of convective instabilities and the edge of the fully stable domain. Hence, this value of S_b will be denoted the local critical wake parameter for convective instabilities, S_{bcc}.

The full range of S_{bcc} values, shown in figure 7, is obtained by a simple method. With the assumption of $\alpha_i = 0$ and $\beta_i = 0$ (i.e. following the abscissa in figure 4), the eigenvalues of S_b, α_r ad β_r are searched for and the neutral curves are illustrated on an (S_b, α_r)-plane. Obviously, when S_b is larger than the maximum value on the neutral curve, the flow will become stable to disturbances. The maximum S_b value is the critical parameter S_{bcc} (see figure 6). The velocity ratio $R = -1.33$ is of interest: here the saddle point has moved down to the abscissa in the $(\alpha_r, -\alpha_i)$-plane, indicating an overlap of the absolute and convective instability points. At yet lower values the spatial amplification rate reverses sign, as shown in figure 8. For $R > -1.33$, the saddle point has negative α_i and therefore the downstream-propagating mode (the lower curve) is spatially growing while the upstream-propagating mode (the upper curve) is spatially damped. But for $R < -1.33$, the saddle point has positive α_i and therefore the upstream-propagating mode is now spatially growing and the downstream-propagating mode is spatially damped. The amplification rate and frequency as functions of R are shown in figure 9.

Furthermore, the frequency of vortex oscillation may be obtained. Koch (1985) and Monkewitz & Nguyen (1987) have shown that for the absolute/convective instability transition in spatially developing flows, a resonance condition may govern the flow. Thus, given a multitude of modes corresponding to different R-values in the near wake, the mode with the maximum amplification rate will be the controlling one. The amplification rate $-\alpha_i$ is shown in figure 9(a) as function of R following the S_{ca} transition line for $R < -0.904$ and then following $S = 0$ for $R > -0.904$. The maximum amplification indeed occurs at the critical point $R = -0.904$. The frequency

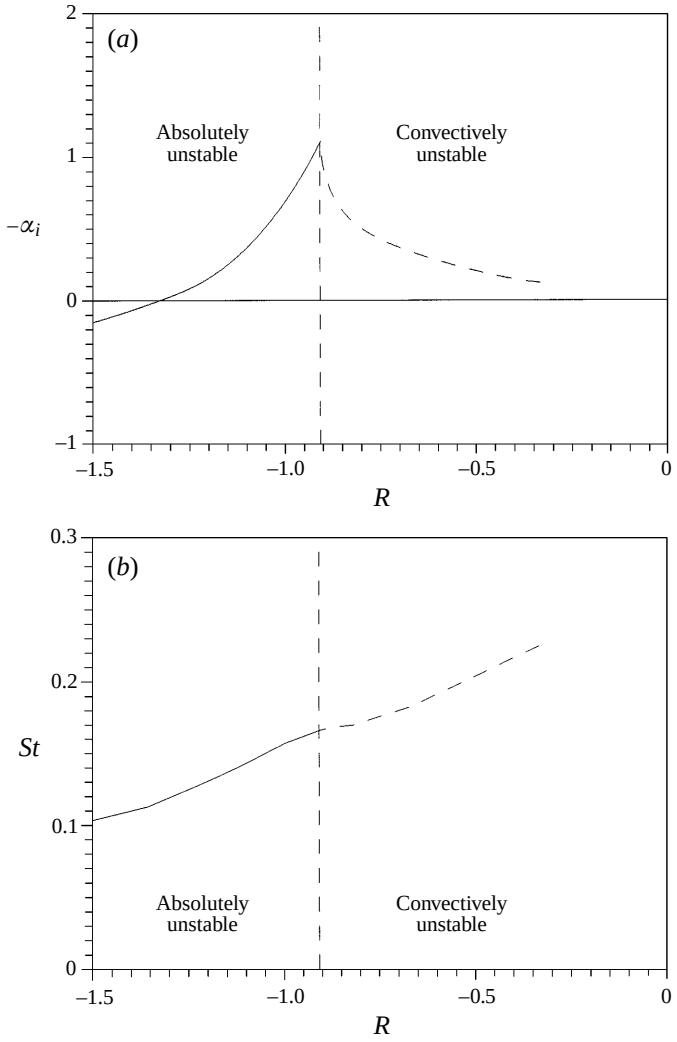

FIGURE 9. Instability properties for the shallow wake: (*a*) amplification rate $-\alpha_i$ as a function of velocity defect R, the absolute/convective instability boundary for $R < -0.904$ and along $S = 0$ for $R > -0.904$; (*b*) corresponding frequency β_r.

of oscillations in the vortex shedding wake is controlled by the value at that critical point $St_b = (\beta_r/2\pi)(2b/U_a) \approx 0.165$ (or $St_d = 0.20$ based on cylinder diameter), as shown in figure 9(*b*).

3. Comparison of experimental results with the instability analysis

The above stability analysis will be compared with the experimental data (mainly the classification of flow patterns) of Chen & Jirka (1995) in this section. The experiments of Morkovin (1964) and stability analysis of Monkewitz (1988) for the unbounded low-Reynolds-number wake are considered as a similar phenomenon.

First, it must be demonstrated that the shallow wake flows are controlled in the main by the turbulent bottom friction (expressed by the wake friction parameter S, or S_b) rather than by lateral turbulent diffusive momentum exchange (expressed by the wake

Reynolds number Re_d, or Re_b). As was shown in figure 5, the flow becomes quite invariant once the local wake Reynolds number $Re_b = U_a 2b/\epsilon_h$ exceeds 1000. A robust estimate for the transverse eddy viscosity in a wide open channel flow is $\epsilon_h = 0.2\, uH$ (Fischer *et al.* 1979) where $u_* = (c_f/2)^{1/2} U_a$ is the shear velocity. Hence, $Re_b \approx (7/c_f^{1/2})$ $(2b/H)$. For the present experiments, with $c_f \leqslant 0.01$ and $(2b)/H \approx D/H \approx 10$ to 100, this givers Re_b of the order of 1000 to 10000. (Yet larger values would hold for actual environmental conditions.) Thus, the turbulent shallow wake can indeed be assumed 'inviscid' (Re_d or $Re_b > 1$) in the sense that small-scale turbulence damping (with scales of the order of H) is negligible. The wake friction parameter S (or S_b) is the single controlling factor.

The present computations of instability are for local instability with the assumption of parallel base flow. In practice, the wake flow will diverge downstream and for the so-called global instability, which allows non-parallel effects, it was found by Chomaz *et al.* (1988) that local absolute instability is a necessary but not sufficient condition for a global mode to become self-excited, i.e. to grow in time. They showed that the region of local absolute instability has to reach a finite critical size before self-excitation (e.g. the Kármán vortex street) is achieved. This means that the onset of the Kármán vortex street occurs as a global transition at a higher Reynolds number than the Reynolds number for the first appearance of local absolute instability. This result has been confirmed by Monkewitz (1988) in his study of low-Reynolds-number unbounded wake flow. He found that $Re_C = 5$ defines the transition of the flow from stability to convective instability, and the absolute instability in the near wake will appear when $Re_d > Re_A = 25$. The strength of the absolute instability grows and finally, when $Re_d > Re_{IK} = 47$, the incipient Kármán vortex street is generated as the end product of absolute instability. Here, the subscript IK means the onset of the incipient Kármán vortex street, A means absolute instability and C means convective instability. Alternatively as Re_d decreases, viscosity will first suppress the vortex shedding when $Re_d < Re_{IK}$, and then, when $Re_d < Re_A$, it will totally damp the absolute instability. For $Re_d < Re_C$, the flow becomes stable.

In the present study, an increase in the bottom friction parameter S will result in a more stable flow (just like decreasing the Reynolds number). The return velocity in the wake flow is the link between the theory (with an assumed velocity profile) and the experiments. As has been discussed, the present study concerns local absolute instability. We now consider the most appropriate velocity profile for representing the global wake characteristics.

Two attempts will be made to do this. First, from the measured maximum return velocity, the R-value in (13) can be determined and critical S-values can be obtained theoretically through figure 6. The maximum return velocity is constant with $U_m/U_a = -0.35$ (or $R = -2.07$) in the unsteady bubble (as shown in figures 1*b* and 1*c*) regime if $S < 0.5$ while there is a rapid decrease of return velocity (R up to -1.1) with increasing S-values within the steady bubble (as shown in figure 1*d*) regime when $S > 0.5$. In order to compare quantitatively the experimental and theoretical results, it is necessary to reconcile the differences in the length-scale definitions of the two wake parameters, S and S_b. From the hot-film measurement of Chen & Jirka (1995), it is found that $2b$ is about $0.82D$. The measured S is thus converted to S_b and results are plotted in figure 10(*a*). One obtains two intersections: 0.65 on the S_{bca} curve and 0.7 on the S_{bcc} curve. The two corresponding critical S-values based on the cylinder diameter are denoted $S_C = 0.85$, characterizing the transition between stability and convective instability, and $S_A = 0.79$, the transition between convective and absolute instability. Experimentally, Chen & Jirka (1995) found $S_V = 0.2$ as the transition

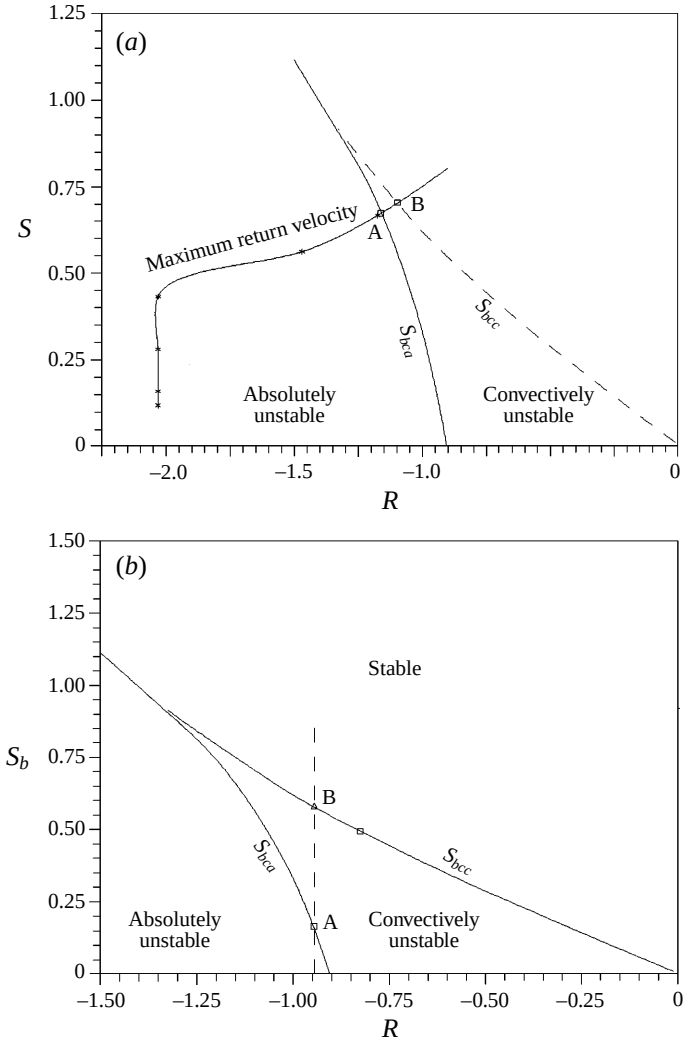

FIGURE 10. Stability diagram for shallow wakes in comparison with experimental data. (*a*) Squares indicate $S_{bca} = 0.65$ and $S_{bcc} = 0.7$ obtained at intersections of lines of critical values on the stability diagram and the $R-S$ relation from experimental return velocities. (*b*) Squares show how measured critical values between different flow patterns correspond to a velocity profile around $R = -0.945$. The triangle is an intersection point of the vertical line of $R = -0.945$ and the S_{bcc} curve.

between vortex shedding and unsteady bubble wake, and $S_U \approx 0.6$ as the transition between an unsteady and steady bubble wake (see table 1). (In fact, an S_U value of 0.5 was quoted by Chen & Jirka. Another inspection shows, however, that a value of 0.6 better approximates the bulk of their data. In any case, inaccuracies in the estimation of the turbulent friction coefficient and inaccuracies in the water depth should be kept in mind here.) The value of S_C dividing wakes with a steady bubble (recirculation zone) and fully unseparated flows at the bottom of table 1 needs to be determined in future, yet larger-scale, laboratory experiments.

In table 1 a comparison has been made between the shallow wake characteristics and the low-Reynolds-number unbounded wake characteristics (Morkovin 1964; Monkewitz 1988). It can be seen that a strong similarity exists between these two kinds

Shallow wake		Unbounded wake	
Observed flow patterns (Chen & Jirka 1995)	Stability analysis (present work)	Observed flow patterns (Morkovin 1964)	Stability analysis (Monkewitz 1988)
Vortex shedding	Absolutely unstable	Vortex shedding	Absolutely unstable
$S_V = 0.2$	—	$Re_K = 90$	—
Unsteady bubble	—	Incipient Kármán vortex	—
$S_U \approx 0.6$	—	$Re_{IK} = 47$	—
—	$S_A = 0.79$	—	$Re_A = 25$
Steady bubble	Convectively unstable	Fixed vortex pair	Convectively unstable
$S_C = ?$	$S_C = 0.85$	$Re_C = 5$	$Re_C = 5$
Unseparated wake	Convectively stable	Unseparated wake	Convectively stable

TABLE 1. Comparison of stability characteristics for shallow wakes and low-Reynolds-number unbounded wakes

of wake instability although there are differences in the physical processes. For increasing S and decreasing Re_d, the suppression of vortex shedding ($S_V = 0.2$ or $Re_K = 90$) and the unstable bubble wake ($S_U \approx 0.6$ or $Re_{IK} = 47$) happen before the damping of the absolute instability ($S_A = 0.79$ or $Re_A = 25$) and convective instability ($S_C = 0.85$ or $Re_C = 5$). Because the vortex shedding is the saturated end product of the absolute instability, there must be a certain level of amplification rate of disturbance to create and maintain vortex shedding. The present result for high-Reynolds-number shallow wakes ($S_C > S_A > S_U > S_V$) is thus equivalent to the sequence for low-Reynolds-number unbounded flow ($Re_K > Re_{IK} > Re_A > Re_C$), reported in Chomaz *et al.* (1988) and Monkewitz (1988). Based on the Squire transformation, two-dimensional disturbance modes as considered herein are more unstable than three-dimensional modes. Naturally, there are some three-dimensional disturbances no matter how strongly two-dimensional the flow may appear to be. This would also partially explain the sequence of ($S_C > S_A > S_U > S_V$).

As the second interpretation of the experimental behaviour, an alternative matching criterion may be based on plotting the measured critical bottom friction stability parameter S_b on figure 6 to obtain the corresponding R-value. The measured values of $S_V = 0.2$ and $S_U \approx 0.6$ based on cylinder diameter can be converted to be 0.164 and 0.492 based on $2b$ and are plotted as square symbols in figure 10(*b*). From $S_V = 0.2$, a corresponding value of R of -0.945 was obtained, which is between the zero return velocity profile of $R = -1$ and the maximum R of the absolutely unstable domain. With $R = -0.945$ an intersection point of $S = 0.7$ (triangle in figure 10*b*) is obtained, which is close to the experimental value of $S_U \approx 0.6$. Following the arguments of Koch (1985) and Monkewitz & Nguyen (1987) for the absolute/convective instability transition in spatially developing flows, a resonance condition may govern the flow. Thus, given a multitude of modes corresponding to different R-values in the near wake, the mode with the maximum amplification rate will be the controlling one. As shown in figure 9, the maximum amplification rate indeed occurs at the critical point $R = -0.904$. Also, as remarked earlier, the frequency of oscillations in the vortex shedding wake is controlled by the critical value of $St_b = 0.165$ or $St_d = 0.20$. This agrees closely with the observed experimental frequency of the vortex shedding wake, $St_b = 0.21$ (Chen & Jirka 1995).

4. Discussion and conclusions

Linear instability analysis of shallow turbulent wake flows has been carried out by using the shallow-water stability (modified Orr–Sommerfeld) equation derived from the depth-averaged shallow-water equations with a term describing bottom friction. Branch-point singularities (indicating absolute instability) have been computed for different wake velocity profiles and absolute and convective instabilities can be suppressed by the bottom friction when the bottom friction stability parameter S is large enough. The amplification rate and frequency were also determined.

The transition values ($S_V = 0.2$ and $S_U \geqslant 0.6$) between different wake flow patterns which have been observed in previous experiments (Chen & Jirka 1995) can be interpreted in the light of the instability analysis. here, S_A corresponds to the instability boundary between absolute and convective instabilities and S_C corresponds to the transition between convectively unstable and stable wake flow. The sequence ($S_C > S_A > S_U > S_V$) corresponds to ($Re_K > Re_{IK} > Re_A > Re_C$) in unbounded low-Reynolds-number flow. Also, the measured values of S_V and S_U were found to correspond to the velocity profile of $R = -0.945$ which appears to be the dominant mode. Another observed property of the wake flow, the Strouhal number of the oscillations, also agrees well with theory.

The present results may also be compared with the stability computations of Grubisic *et al.* (1995) for the shallow wake behind mountains in a stratified atmosphere. Their stability equation is similar to the present one. The application of a piecewise-linear (triangular) velocity profile misses the two inflection points, however. Their result gives a critical 'surface drag number' r (numerically about one half of S as defined herein) of about 0.10. Their results, just like the present ones, explain the vortex shedding wakes as observed in the majority of atmospheric cases, but are not in agreement with the stable bubble wake for the mountain island of Hawaii (Smith & Grubisic 1993). The presence of internal hydraulic jumps with additional energy dissipation and internal wave radiation may account for these discrepancies. Clearly, additional work including the range of other dissipative mechanisms will be needed to explain the full behaviour of these diverse types of shallow flows in the natural environment.

The project was undertaken at Cornell University. Support by the US National Science Foundation (Grant No. MSM-8806130) and the Electric Power Research Institute (Grant No. RP8006-15) is gratefully acknowledged. The instability computations were carried out with the facilities of the Cornell National Supercomputer Facility supported by the National Science Foundation. The assistance of Professor P. K. Stansby in the preparation of this manuscript is gratefully acknowledged.

REFERENCES

Bers, A. 1975 Linear waves and instabilities. In *Physique des Plasmas* (ed. C. Dewitt & J. Peyraud), p. 117. Gordon and Breach.

Betchov, R. & Criminale, W. O. 1966 Spatial instability of the inviscid jet and wake. *Phys. Fluids* **9**, 359.

Briggs, R. J. 1964 *Electron-Stream Interaction with Plasmas*. MIT Press.

Castro, I. P. & Haque, A. 1987 The structure of turbulent shear layer bounding a separation region. *J. Fluid Mech.* **179**, 439.

Chen, D. & Jirka, G. H. 1993 Flow visualization and absolute instability analyses for plane wakes bounded in a shallow water layer. In *Advances in Hydro-Science and Engineering* (ed. S. Y.

Wang), vol. 1, p. 1124. Center for Computational Hydroscience and Engineering, The University of Mississippi.

CHEN D. & JIRKA, G. H. 1994 Linear instability of the annular Hagen–Poiseuille flow with small inner radius by a Chebyshev pseudo-spectral method. *Intl J. Comput. Fluid Dyn.* **3**, 265.

CHEN, D. & JIRKA, G. H. 1995 Experimental study of plane turbulent wake in a shallow water layer. *Fluid Dyn. Res.* **16**, 11.

CHOMAZ, J. M., HUERRE, P. & REDEKOPP, L. G. 1988 Bifurcations to local and global modes in spatially developing flows. *Phys. Rev. Lett.* **60**, 25.

CHOMAZ, J. M., HUERRE, P. & REDEKOPPP, L. G. 1991 A frequency selection criterion in spatially developing flows. *Stud. Appl. Maths* **84**, 119.

CHU, V. H., WU, J. H. & KHAYAT, R. E. 1991 Stability of transverse shear flows in shallow open channels. *J. Hydraul. Engng* **117**, 1370.

ETLING, D. 1989 On atmospheric vortex streets in the wake of large islands. *Met. Atmos. Phys.* **41**, 157.

FISCHER, H. B., LIST, E. J., KOH, R. C. Y., IMBERGER, J. & BROOK, N. H. 1979 *Mixing in Inland and Coastal Waters*. Academic.

GERRARD, J. H. 1978 The wake of cylinder bluff bodies at low Reynolds number. *Phil. Trans. R. Soc. Lond.* A **288**, 351.

GRUBISIC, V., SMITH, R. B. & SCHAR, C. 1995 The effect of bottom friction on shallow-flow past an isolated obstacle. *J. Atmos. Sci.* **48**, 1985.

HUERRE, P. & MONKEWITZ, P. A. 1990 Local and global instabilities in spatially developing flows. *Ann. Rev. Fluid Mech.* **22**, 473.

INGRAM, R. G. & CHU, V. H. 1987 Flow around islands in Rupert Bay: An investigation of the bottom friction effect. *J. Geophys. Res.* **92**, 14521.

KOCH, W. 1985 Local instability characteristics and frequency determination of self-excited wake flows. *J. Sound Vib.* **99**, 53.

MATTINGLY, G. E. & CRIMINALE, W. O. 1972 The stability of an incompressible two-dimensional wake. *J. Fluid Mech.* **51**, 233.

MONKEWITZ, P. A. 1988 The absolute and convective nature of instability in two-dimensional wakes at low Reynolds number. *Phys. Fluids* **31**, 999.

MONKEWITZ, P. A. & NGUYEN, L. N. 1987 Absolute instability in the near-wake of two-dimensional bluff bodies. *J. Fluids Struct.* **1**, 165.

MORKOVIN, M. V. 1964 Flow around circular cylinder-kaleidoscope of challenging fluid phenomena. In *Proc. Symp. Fully Separated Flows*, p. 102. ASME, Philadelphia.

OERTEL, H. 1990 Wakes behind blunt bodies. *Ann. Rev. Fluid Mech.* **22**, 539.

PATTIARATCHI, C., JAMES, A. & COLLINS, M. 1986 Island wakes and headland eddies: A comparison between remotely sensed data and laboratory experiments. *J. Geophys. Res.* **92**, 783.

ROSHKO, A. 1961 Experiments on the flow past a circular cylinder at high Reynolds number. *J. Fluid Mech.* **60**, 345.

SCHAR, C. & SMITH, R. B. 1993 Shallow-water flow past isolated topography. Part II: Transition to vortex shedding. *J. Atmos. Sci.* **50**, 1401.

SCORER, R. S. 1978 *Environmental Aerodynamics*. Ellis Horwood.

SMITH, R. B. & GRUBISIC, V. 1993 Aerial observations of Hawaii's wake. *J. Atmos. Sci.* **50**, 3728.

VAN DYKE, M. 1982 *An Album of Fluid Motion*. Parabolic Press.

WOLANSKI, E. J., IMBERGER, J. & HERON, M. L. 1984 Island wakes in shallow coastal waters. *J. Geophys. Res.* **89**, 10553.

YU, M.-H. & MONKEWITZ, P. A. 1988 Self-excited oscillations in a low-density two-dimensional jet. *Bull. Am. Phys. Soc.* **33**, 2246.